



---

*Research article*

## **Bioelectricity production from anaerobically treated leachate in microbial fuel cell using *Delftia acidovorans* spp.**

**Cristina Calderón-Tapia<sup>1,\*</sup>, Daniel Chuquín-Vasco<sup>2</sup>, Alex Guambo-Galarza<sup>1</sup>, Soledad Núñez-Moreno<sup>3</sup> and Cristina Silva-Cisneros<sup>4,5</sup>**

<sup>1</sup> Escuela Superior Politécnica de Chimborazo (ESPOCH), Research and Development Group for the Environment and Climate Change (GIDAC), 060101 Riobamba, Ecuador

<sup>2</sup> Escuela Superior Politécnica de Chimborazo (ESPOCH), Chemical Engineering Career, Safety, Environment and Engineering Research Group (GISAI)

<sup>3</sup> Escuela Superior Politécnica de Chimborazo (ESPOCH)

<sup>4</sup> Institute Research Centre for Natural Sciences, Eötvös Loránd Research Network (ELKH), Budapest, Hungary

<sup>5</sup> Department of Physical Chemistry and Materials Science, Faculty of Chemical Technology and Biotechnology, Budapest University of Technology and Economics, Budapest, Hungary

\* **Correspondence:** Email: [cristina.calderont@epoch.edu.ec](mailto:cristina.calderont@epoch.edu.ec); Tel: +593998724006.

**Abstract:** Microbial fuel cells (MFCs) are devices that use microorganisms to produce electricity from organic matter. In this study, the bacterium *Delftia acidovorans* spp was used to evaluate energy generation in a single-chamber MFC. In this evaluation, six MFCs were assembled with different exchange membranes: two with carbon fiber composite membrane, two with maghemite membrane and two with heat-treated maghemite. Synthetic maghemite was characterized using X-ray powder diffraction (XRD), X-ray photoelectron spectroscopy (XPS), Brunauer-Emmett-Teller (BET) and Fourier transform infrared spectroscopy (FTIR) measurements. Bioelectricity monitoring in the MFCs was conducted for 15 days, with data collected every 60 seconds. The cell that achieved the highest bioelectricity production was the one with heat-treated maghemite, reaching a production of 286.50mV. It used 100% leachate from fruit and vegetable waste as a substrate, starting with values of 365 mg/L of N-NH<sub>4</sub>, 96000 mg/L of biochemical oxygen demand (BOD<sub>5</sub>), 101500 mg/L of chemical oxygen demand (COD) and a pH of 4.11. In the results, the carbon fiber treatment had a higher removal efficiency percentage of up to 63.38% for BOD<sub>5</sub> and 69.67% for COD. For ammonium nitrogen removal, all cells showed good removal efficiency of up to 92.49%. The pH value increased in all

treatments due to the degradation of organic matter, reaching a value of up to 5.96. Thus, the efficiency of *Delftia acidovorans* spp. and carbon fiber are a good alternative as an exchange membrane in purifying leachate contaminants within an MFC.

**Keywords:** microbial fuel cell (MFC); *Delftia acidovorans* spp; leachate treatment; maghemite

---

## 1. Introduction

All development processes are based on energy, and most human activities utilize fossil fuels for their advancement [1]. However, we must understand that this type of fuel is being depleted and we need to develop alternative energies. Currently, the use of solar panels, wind turbines, geothermal energy and microbial fuel cells are being investigated as sustainable alternatives for energy production [2,3]. Microbial fuel cells (MFCs) are devices that use microorganisms to produce electricity from organic matter [4,5]. The operation of MFCs is based on the use of one or two chambers, one aerobic and the other anaerobic [6,7]. In the anodic anaerobic chamber, the effluent to be treated enters. The effluent is then oxidized by electrogenic microorganisms that use electron acceptors such as nitrates ( $NO_3^-$ ), ferric ions ( $Fe^{3+}$ ), sulfates ( $SO_4^{2-}$ ), carbonates ( $CO_3^{2-}$ ) and certain organic compounds, excluding oxygen. [8,9]. The cathodic aerobic chamber is exposed to atmospheric air. Dissolved oxygen is reduced to form electrons that move towards the cathode, and the protons produced in the anodic chamber diffuse through the membrane in proportion to the cathodic chamber via an external circuit, forming water[10].

This process generates bioelectric power through the flow of electrons to the cathode in an external circuit regime [4]. In this process, electrogenic bacteria metabolize organic substrates by transferring electrons to the external electrode. The electron transfer phenomenon is due to the electrogenic capability of bacteria to donate electrons to a solid electron acceptor during anaerobic respiration [2,11]. The most commonly used electrogenic bacterial communities in microbial fuel cells are *Proteobacteria*, *Firmicutes*, *Bacteroidetes*, *Actinobacteria*, *Aquificae*, *Acidovorax*, *Soehngenia*, *Clostridium*, *Sulfurihydrogenibium*, *Flexibacter* and *Mycobacterium* [5,12–14]. In this diversity, the bacterium *Delftia acidovorans* has been cited only once for a study comparing microbial fuel cells with aerobic and anaerobic anodes [15].

On the other hand, the use of electrogenic bacteria within an MFC are environmentally conscious options because while they generate bioelectricity, they can also collaborate in the following processes for example:wastewater treatment [16], bioprocesses [17], removal of compounds such as dyes [18], contaminants such as glyphosate [19], hydrocarbon degradation [20,21] and for the treatment of leachates where upto 37% COD removal efficiency was obtained [22].

The performance of an MFC can be influenced by the cell design [23] and the type of exchange membrane used [24]. Nafion is the most common material in this type of cell, but it is expensive, can result in slow proton transfer and increased internal resistance due to fouling [25]. This obstacle can lead to a decrease in pH in the anodic chamber, influencing bacterial development and system stability [26]. As an alternative to Nafion, other materials have been tested, such as polypropylene, propylene sulfide, cellulose esters and cation exchange separators, generating voltages between  $0.387 \pm 0.005$  and  $0.483 \pm 0.006$  V comparable to those obtained with Nafion [27]. Another material used for proton transport to the cathode is carbon fiber, which exhibits excellent properties such as

microscale diameter, high hardness, high strength, lightweight and resistance to high temperatures [28–31]. It also performs well in a single-chamber MFC, resulting in higher bioelectricity production than a double-chamber MFC [32]. In a previous study [8], a single-chamber MFC with carbon fiber as an exchange membrane was used to treat organic waste from fruits and vegetables, achieving an average of continuous current of 330 volts.

However, surface modification of carbon fibers has become an interesting research area. Heteroatoms and carbon-based catalysts co-doped with transition metals such as iron, nitrogen and sulfur are used to enhance the catalytic activity of the oxygen reduction reaction (ORR) by increasing surface roughness [29,33]. In one study, natural maghemite (NM), which is abundant in the earth, was used to activate peroxydisulfate (PDS) in an electrolytic cell for the oxidation of acid orange 7 (AO7), achieving a removal efficiency of over 90% [34]. This maghemite system could be a promising candidate for treating organic wastewater. Therefore, in this study, we evaluated the production of bioelectricity and the degradation of leachates using a single-chamber MFC with carbon fiber as the exchange membrane, supplemented with laboratory-synthesized maghemite. The maghemite was synthesized using the bacterium *Delftia acidovorans*, isolated from the soil of the Ecuadorian paramo.

## 2. Materials and methods

### 2.1. Microbial analysis of *Delftia acidovorans* spp.

The isolation and characterization of the bacteria was performed to construct the microorganisms bank of the Biological Sciences Laboratory of the Faculty of Natural Resources of ESPOCH. For the activation of *Delftia acidovorans*, it was seeded on liquid media with 0.19 g of nutrient agar (Merck) and distilled water. Next, the amount was divided into six test tubes, inoculated 2 mL of bacteria in each one and then stored at 28°C for 48 hours [35]. In the laboratory of the GIDAC research group at ESPOCH University in Ecuador, a bank of microorganisms is isolated from the soil of the Ecuadorian paramo. The characterization of this material is important to find their potential uses in biotechnology and bioremediation, and we decided to use the bacterium *Delftia acidovorans* to evaluate its bioelectricity production and leachate degradation.

The bacterium was isolated from the paramo land, and the molecular identification was stored in bank microorganism that belongs to ESPOCH. After the activation process, the bacteria were identified by Gram staining. For molecular identification, once the DNA was extracted, DNA amplification was carried out using universal primers 27F/1492R (5'-AGAGTTTGATCCTGGCTCAG-3'/5'-GGTACCTTGTTACGACTT-3') [36], targeting the bacterial 16S rRNA gene region. Sequences were analyzed as described in the study by Geer L Y et al. [37] using the Geneious R9.1 program and with the assistance of the NCBI database. In Table 1, the comparison of the GenBank database of the bacteria is reported.

**Table 1.** Molecular identification of *Delftia acidovorans* spp.

| Original code | Length of the fragment | % Quality of the fragment | Organism                   | Fragment | % Specie identity | N° of Accession            |
|---------------|------------------------|---------------------------|----------------------------|----------|-------------------|----------------------------|
| A140          | 403 pb                 | 61.5                      | <i>Delftia acidovorans</i> | 16S      | 99.26             | <a href="#">LC462156.1</a> |

## 2.2. Leachate characterization

Leachate was sampled from the market EP-EMMPA San Pedro located in Riobamba, Ecuador. The considered daytime for sampling was in the afternoon at 14:00 due to the greater influx of stevedores. The waste sample weighed 3 kg, consisting of fruits and vegetables in a 50:50 ratio, i.e., 1.5 kg of fruit waste, such as banana, tangerine, orange or papaya, and 1.5 kg of vegetables, such as radish, carrot, tomato or bell pepper. The waste was shredded and mixed to facilitate leachate extraction.

Leachate collection involved simulating precipitation from January to August 2022, totaling 3.21 mm, based on data from the ESPOCH university meteorological station. This calculation used the standard area of a waste container measuring 0.171 m<sup>2</sup>, with a capacity of 65 kg. Employing these parameters, we added 0.549 L of rainwater and obtained 1.5 L of leachate, which served as the substrate for the MFCs.

Following, a leachate sample was taken to determine: the ammoniacal nitrogen 4500-NH<sub>4</sub>-C [38], BOD<sub>5</sub> standard method 5210-B [39], COD colorimetric method 5220-D [40] and pH analysis 4500-H-B [41].

## 2.3. Synthesis of maghemite

The synthesis of maghemite nanoparticles was based on the mixture of FeCl<sub>3</sub>·6H<sub>2</sub>O and FeCl<sub>2</sub>·4H<sub>2</sub>O in a ratio (2:1) with 50 mL of deionized water to obtain 2M solution of ferric chloride and 1M of ferrous chloride [42]. Next, 27.86 g of ferric chloride was placed in a beaker with 9.94 g of ferrous chloride and then continuously mixed at 70°C. On the other hand, 12 g of sodium hydroxide (NaOH) and 200 mL of deionized water were mixed in a volumetric flask. Next, the sodium hydroxide solution was added dropwise to the mixture of iron chlorides. This mixture was maintained under nitrogen for approximately 2 hours, facilitating the formation of black lumps that visually reflected the effectiveness of the synthesis. At the end, pH was measured, obtaining alkalinity results in the solution. Finally, the supernatant of the sample was removed, and the obtained precipitate was washed with 250 mL of ethanol and centrifuged at 3000 rpm for 10 minutes; once the time elapsed, a second wash was carried out with 1L of deionized water. Then, the sample was centrifuged again at 3000 rpm for 10 min. The supernatant was discarded, and the sample was collected and dried in a muffle for 3 days at room temperature. The sample was weighed, obtaining 10 g of iron oxide. For the treated sample, part of the final product was taken into the muffle at 100°C for 3 hours.

## 2.4. Characterization of maghemite

### 2.4.1. Phase composition and morphology

Samples in the original and low treatment state were characterized by X-ray diffraction patterns using a Philips model PW 3710 based PW 1050 Bragg–Brentano parafocusing goniometer with CuK $\alpha$  radiation, graphite monochromatic and proportional counter.

#### 2.4.2. X-ray photoelectron spectroscopy

Surface analysis was conducted by X-ray photoelectron spectroscopy (XPS) using an Omicron EA 125 electron spectrometer operated in the constant analyzer energy mode (pass energy 30 eV, resolution around 1 eV) with a AlK $\alpha$  (1486.6 eV) radiation as excitation source. A detailed description of the system can be found in previous studies [43,44]. Then, the spectra of the samples were recorded (Fe 2p, Cl 2p, Na 1s, C 1s, O 1s). The spectra were processed with the software Casa XPS [45] by fitting the data with a combination of Gaussian–Lorentzian peaks with linear and Shirley background [46]. The quantitative analysis was performed with the software XPS MultiQuant [47,48] assuming a homogeneous distribution of the components.

#### 2.4.3. BET: Brunauer-Emmett-Teller analysis

Nitrogen adsorption measurements were carried out at temperature of liquid nitrogen using Thermo Scientific Surfer automatic volumetric adsorption analyzer (Thermo Fischer Scientific, Berlin, Germany). The specific surface area is interpreted according to the BET method in the range of relative pressures from 0.05 to 0.30.

#### 2.4.4. FTIR characterization

Fourier transform infrared spectroscopy (FTIR) measurements were performed by collecting the IR spectra using a Varian Scimitar 2000 FT-IR spectrometer (Varian Inc, US) using attenuated total reflection (ATR) technique. The solid samples were positioned and pressed (70 cNm) by a sapphire anvil to promote contact between the sample and diamond surface.

### 2.5. MFCs construction and operation

An MFC converts organic matter into electrical energy. The design used in this experiment was a simple configuration, composed of a single chamber divided into an anodic section and a cathodic section joined through proton exchange membranes. In the anodic section, bacteria donate electrons, whereas in the cathodic section, electrons are transferred to a final electron acceptor [12]. Electrogenic bacteria can release electrons to the anode through the oxidation of organic compounds. In this study, leachate produced from vegetable waste was used as a source of organic matter. The generated electrons flow through an external circuit containing an external resistance to the cathode. The electron flow is governed by the electrochemical potential between the final bacterial respiratory enzyme and the cathode electricity acceptor [49]. In the internal circuit, protons diffuse from the anode to the cathode through a proton-permeable membrane. The membranes used in this experiment were carbon fiber, maghemite and maghemite with heat treatment, covered with cellophane paper. At the cathode, electrons and protons combine to reduce the terminal electron acceptor, which in our case is oxygen. The carbon fiber membrane used is a commercial carbon fiber composite, primarily composed of clustered carbon filaments impregnated with resin. The membrane is manufactured through controlled pyrolysis of polyacrylonitrile (PAN) as the precursor.

The anodic section is formed by a transparent acrylic cylinder with a square base of  $7.5 \times 7.5$  cm, a diameter of 50 mm, a height of 63.6 mm and a 13 mm hole in the cylinder wall to feed the substrate.

On the other hand, the cathodic section consists of a lower acrylic plate with two lines and an upper one with three lines. Moreover, the membranes introduced between the acrylic plates were 0.8mm thick carbon fiber and 2g of maghemite. The carbon fiber membranes were treated according to a previously proposed protocol [50]. The experiment was divided according to the proton exchange membrane (Table 2).

**Table 2.** Description of the treatments performed in the MFC.

|                          |  |                       |                       |
|--------------------------|--|-----------------------|-----------------------|
| Treatment 1<br>(MFC 3_1) | Cell with carbon fiber   | Repeat 1 – MFC<br>1-1 | Repeat 2 – MFC<br>2-1 |
| Treatment 2<br>(MFC 3_2) | Cell with carbon fiber + maghemite (sample B)                  | Repeat 1 – MFC<br>1-2 | Repeat 2 – MFC<br>2-2 |
| Treatment 3<br>(MFC 3_3) | Cell with carbon fiber + maghemite low heat treated (sample A) | Repeat 1 – MFC<br>1-3 | Repeat 2 – MFC<br>2-3 |

## 2.6. Power generation

Monitoring and storage of voltage data, generated by the MFCs, was obtained through a data acquisition system using an Arduino [51] composed of three converters that operated under a digital data collection model, executed by the LabView software, which recorder the data in intervals of 60 s for 15 days, complying with the 24-hr cycles to obtain a global voltage average [52].

The experimental analysis considered leachate (dependent variable) to understand the effect of MFC on *Delftia acidovorans* spp. (independent variable). Statistical analysis of the data showed a normal distribution with 95% confidence interval. ANOVA parametric test was used to evaluate the variation between treatments. Tukey HSD test ( $P \leq 0.05$ ) [53] was used to make multiple comparisons and evaluate the qualitative variables, which allowed determining the significant differences between the treatments: Treatment 1 (MFC 3\_1), Treatment 2 (MFC 3\_2) and Treatment 3 (MFC 3\_3) using the SPSS 22.0 software.

## 3. Results and discussion

### 3.1. Leachate analysis

The amount of leachate generated in landfills can range from 15–50% of their total volume [54] and contains contaminants such as dissolved organic matter, xenobiotics, heavy metals and inorganic compounds [55]. In the determination of the contamination amount removed from the leachate, first determination of BOD<sub>5</sub>, COD, ammonia nitrogen and Ph were measured to identify the initial values before the treatment. After the treatment in MFC the same measurements were performed to evaluate the difference in the values [56]

Figure 1 shows the efficiency of removal of ammoniacal nitrogen in the different treatments. The concentration of ammonia nitrogen at the beginning was 365.0 mg/L, and during the process of oxidation of the organic matter decreased 27.4 mg/L in MFC 1-1 and 30.14 mg/L in MFC 2-1 (both composed with carbon fiber), showing the highest efficiency compared to the other treatments. The cell with maghemite and maghemite with thermal treatment and carbon fiber exhibits the lowest efficiency where the degradation of ammonia nitrogen in MFC 2-2 is 48.63 mg/L and in MFC 1-3 is

61.64 mg/L. The ANOVA study showed a p-value greater than 0.05, suggesting that there were no significant differences between the treatments. Therefore, it can be generally stated that all treatments have a good removal efficiency greater than 83%, similar to the results obtained with MFC, where a removal efficiency of 70% to 90% was achieved [57,58]. In a previous study [59], it was determined that ammonia in a substrate increases energy production up to a certain point. If the limit is exceeded, ammonia ions have an inhibitory effect and reduce energy production. However, in this study, no inhibition reducing energy production was observed during the measurement.

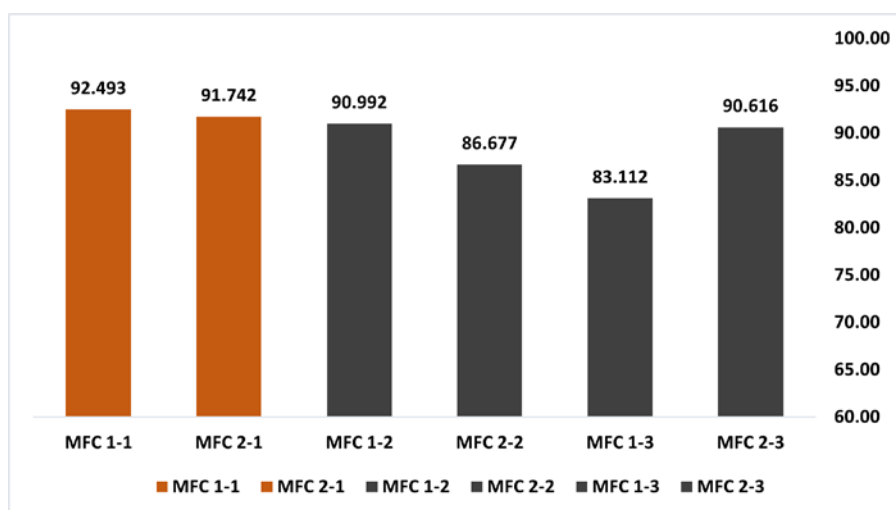


**Figure 1.** Percentage removal of N-NH<sub>4</sub> (mg/L) in each experiment.

In the case of COD, Figure 2, the amount of dissolved oxygen in the substrate, i.e. oxidation of the organic matter, the initial value was 101500 mg/L and after 15 days a similar decrement was observed between MFC 1-1 (31280 mg/L) and MFC 2-1 (30790 mg/L); for MFC 1-2 the degradation decreases to 64.09% (36450 mg/L) and for MFC 2-2 was 58.75% (41870 mg/L). In the case of MFC 1-3 and MFC 2-3 the biomass degradation was inferior to the other treatments with 55.60% (45070 mg/L) and 60.93% (39660 mg/L), respectively. According to the ANOVA study, a p-value less than 0.05 was obtained, suggesting significant differences between the treatments. The results indicate that the added maghemite does not favor COD removal in the substrate. It is important to mention that in this study, 100% leachate was used. When comparing these results with a previous study [59], where they obtained an approximately 49% removal rate, we can observe that using carbon fiber as a membrane results in significant removal, and the efficiency percentage decreases in cells where maghemite was used around 55.60%.

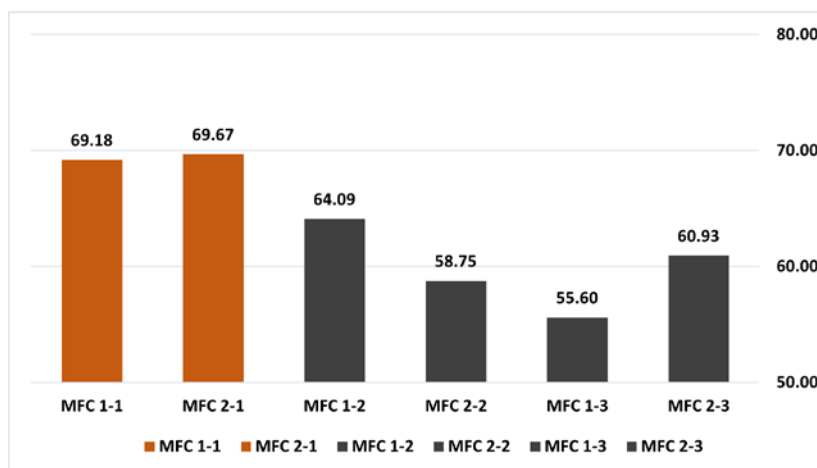


**Figure 2.** Percentage removal of COD (mg/L) in each experiment.

Regarding BOD<sub>5</sub>, Figure 3 shows an initial value of 96000 mg/L with a BOD<sub>5</sub>/COD ratio of 0.95. This ratio exceeds 0.5 indicating a high concentration of biologically degradable matter. Such elevated concentrations promote degradation activity and bioelectricity production, which is advantageous[58]. According to the ANOVA study, a p-value less than 0.05 was obtained, suggesting significant differences between the treatments. The results indicate that the high percentage of degradation belongs to the carbon fiber MFC 2-1 with 63.38% (35160 mg/L) following by MFC 1-2 with a removal efficiency of 58.50% (39840 mg/L). For MFC 2-2, MFC 1-3 and MFC 2-3, there was low BOD<sub>5</sub> removal of 2.34% (93750 mg/L), 0.72% (95310 mg/L) and 11.57% (84890 mg/L) respectively. Agreeing that the cells where maghemite is added to the membrane decrease the percentage of removal of these contaminants.

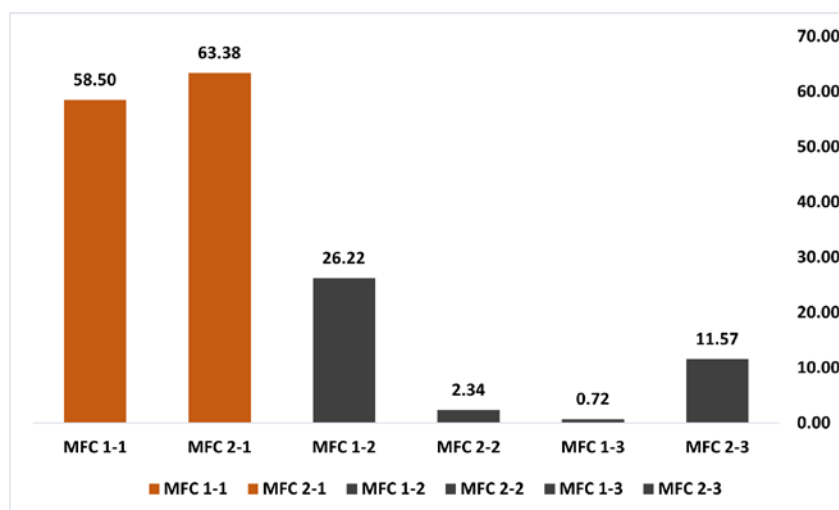


**Figure 3.** Percentage removal of BOD<sub>5</sub> (mg/L) in each experiment.

In Figure 4, the pH measurement was evaluated every day in each MFC. The initial value was 4.11, but during the 15 days of the experiment the leachate showed increasing pH until the last day of monitoring. The final pH of the samples was 4.46 for MFC 1-1, 4.65 for MFC 2-1, 4.86 for MFC 1-2, 4.84 for MFC 2-2, 5.78 for MFC 1-3, 5.96 for MFC 2-3. The importance of pH in the efficiency of



MFC is well known. Proton transfer is affected at low pH, and as pH increases, bioelectricity production also increases. However, if the pH is too high, it can also affect proton transfer [60]. In this study, an increase in pH is observed over the days as a result of the degradation of organic matter and the increase in bioelectricity production without affecting proton transfers.

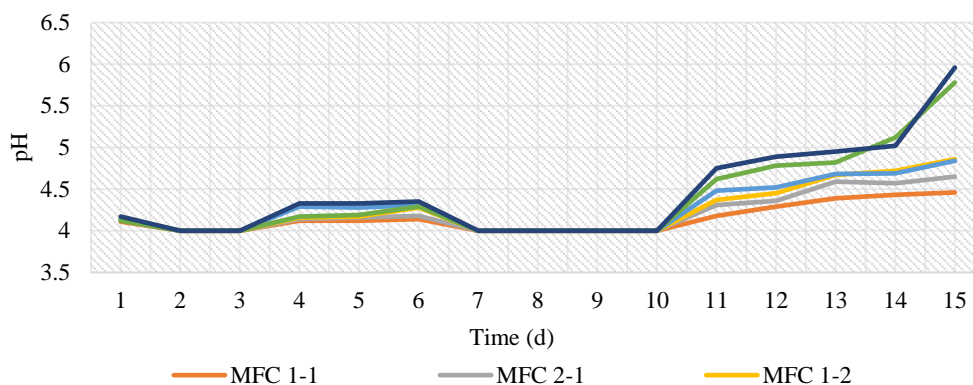


**Figure 4.** Monitoring of pH during the experimental period.

### 3.2. Characterization of maghemite

The X-ray powder diffraction (XRD) diffractograms for the two samples of synthesized maghemite samples are shown in Figure 5. In general, all diffractograms showed line broadenings (crystallographic identification was done using the PDF card # 39–1346 52 Magh for  $\gamma\text{-Fe}_2\text{O}_3$  compared in XDB software with bauxite data base). The main diffraction peaks are related to pure maghemite phase [61] observed at  $2\theta = 30.2, 35.6, 43.3, 53.7, 57.3$  and  $62.9$  from the (220), (311), (400), (422), (511) and (440) crystallographic planes compound. In Table 1, the experimental data of the two samples is shown, where the difference in the peak position is negligible. It has been observed that the calculated d-spacing values are very close to maghemite standard values. However, the data evaluation in the software XDB suggest maghemite phase. The average crystallite size calculated using Debye-Scherrer's equation was 12.17 nm and 8.41 nm for B and A samples, respectively.

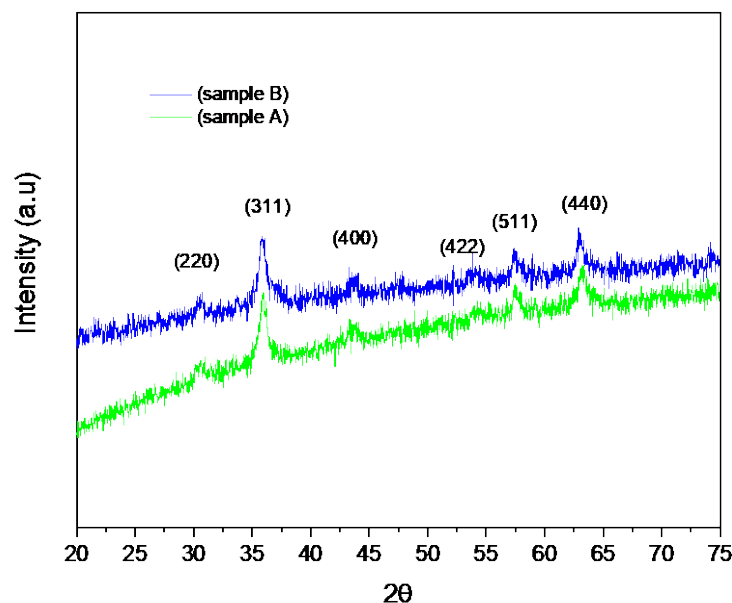


**Figure 5.** XRD diffraction patterns of iron oxide powder of the parent sample (B: no treatment) and low heat-treated sample (A: 100°C for 3 hours).

Nitrogen surface adsorption isotherms for the samples had similar shape and were assigned to type II with H3 type of hysteresis. Additionally, the Brunauer-Emmett-Teller (BET) surface areas of the samples were measured. For sample B  $\sim 104.64 \text{ m}^2/\text{g}$  and for the sample A  $\sim 97.74 \text{ m}^2/\text{g}$ . Total pore volume was  $0.2857 \text{ cm}^3/\text{g}$  for sample B and  $0.2691 \text{ cm}^3/\text{g}$  for the sample A. Similar results were found where the range of BET surface area was  $\sim 27$  to  $149.8 \text{ m}^2/\text{g}$  [62]. When sample A is treated at low temperature, according to the study of Trushkina Y et al. [63], the 100 °C treatment is not enough to demonstrate a structural change in the system.

**Table 3.** Standard XRD data for standard maghemite and the obtainer powder.

| Standard data      |              | Experimental data Sample B |              | Experimental data Sample A |              |
|--------------------|--------------|----------------------------|--------------|----------------------------|--------------|
| Pos. ( $2\theta$ ) | $d$ -spacing | Pos. ( $2\theta$ )         | $d$ -spacing | Pos. ( $2\theta$ )         | $d$ -spacing |
| 30.26              | 2.953        | 30.3149                    | 2.9460       | 30.1144                    | 2.9652       |
| 35.66              | 2.518        | 35.8129                    | 2.5053       | 35.9299                    | 2.4974       |
| 43.37              | 2.086        | 43.2995                    | 2.0879       | 43.3329                    | 2.0864       |
| 53.78              | 1.704        | 53.8443                    | 1.7013       | 53.9613                    | 1.6979       |
| 57.32              | 1.607        | 57.5041                    | 1.6014       | 57.9613                    | 1.5898       |
| 62.98              | 1.476        | 62.9019                    | 1.4763       | 63.0689                    | 1.4728       |

The FTIR spectra is showed in the Figure 6, where the peaks around  $1600 \text{ cm}^{-1}$  correspond to the O-H groups and those around  $1400 \text{ cm}^{-1}$  correspond to C-O bonds. The peaks at low frequency from  $410 \text{ cm}^{-1}$  to  $630 \text{ cm}^{-1}$  are related to the iron oxide compounds. The hydroxyl O-H group presented around  $3100\text{-}3600 \text{ cm}^{-1}$  represent the evidence of OH group of water [61]. Peak around  $400 \text{ cm}^{-1}$  corresponding with vibration in octahedral site of the Fe–O bond which is consistent with those for the spinel maghemite ( $\gamma\text{Fe}_2\text{O}_3$ ) phase [64,65]. Those peaks are clearly visible because the product is

crystalline. The presence of the maghemite phase is in good agreement with the synthesis procedure, which the oxidation salt mixture to  $\text{Fe}_2\text{O}_3$  is likely to occur.

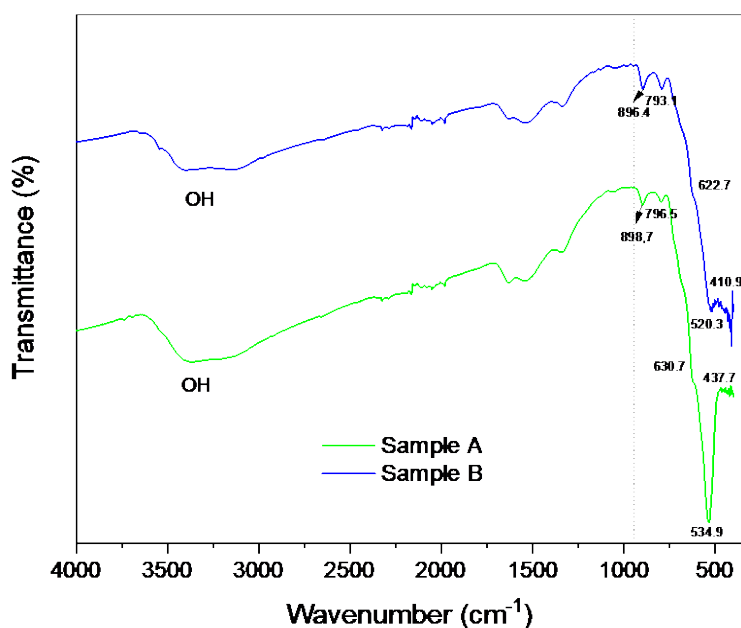


**Figure 6.** FTIR spectra of the parent sample (B: no treatment) and low heat-treated sample (A: 100°C).

An XPS measurement was performed in order to identify the synthesized sample from the pure maghemite chemical composition ( $\gamma\text{-Fe}_2\text{O}_3$ ), which is showed in the Figure 7. The full scanning of the sample A and the specific Fe 2p (panel a) is showed with Al source excitation in the range of 0 to 1486.6 Ev. According with the literature [66], the Fe 2p<sub>3/2</sub> spectra (Fig. 3a) exhibit two peaks at 710.4 and 724.1 Ev, which are very close to the  $\text{Fe}^{3+}$  spectra of  $\gamma\text{-Fe}_2\text{O}_3$  sample at 100 °C. Therefore, the XPS results are in a good agreement with the XRD results.

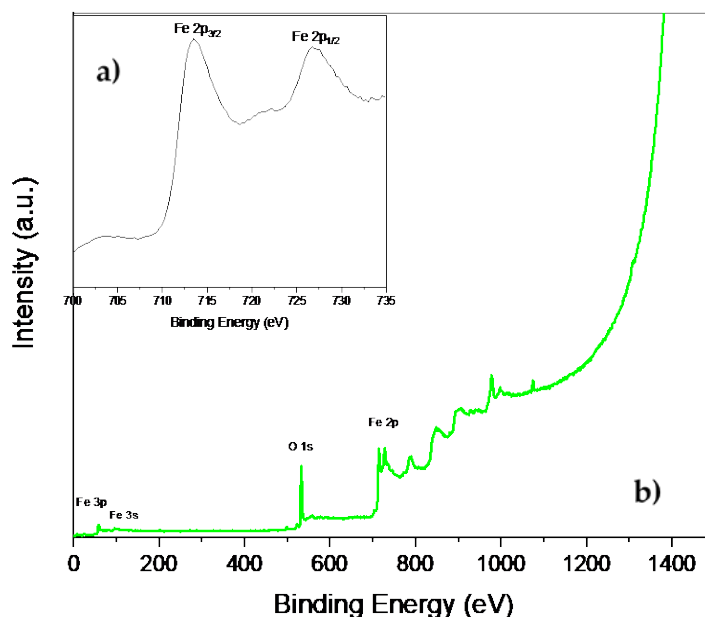


**Figure 7.** XPS spectra of  $\gamma$ -Fe<sub>2</sub>O<sub>3</sub> nano-particles of the sample heat treated at low temperature. (a) XPS spectra of Fe 2p core-level, (b) Full scanned XPS spectra.

### 3.3. Operation of the MFCs

The species *Delftia* belongs to the *Comamonadaceae* family of *Betaproteobacteria* [67]. *Delftia 858cidovorans* is a Gram-negative microorganism that has been isolated from water, soil, and hospitals. Reports so far suggest that the bacterium has the ability to degrade various organic and inorganic compounds and may exhibit an alternative anaerobic metabolism, such as nitrate reduction, making it a potential candidate for use in MFCs [68–70]. In the study by Nosek D et al. [71], *Betaproteobacteria* were identified as the most abundant class-level group on MFC anodes. Additionally, both Ishii S et al.[72] and Chen C Y et al.[15] detected the presence of *Delftia* in their MFC anodes. However, this evidence alone is insufficient to categorize *Delftia* as an electrogenic bacterium, suggesting the need for further studies. In 2016, [73] used a strain of *Delftia* isolated from a fractured rock aquifer as a pure culture in a half-cell reactor, comparing it to another specimen from the German Collection of Microorganisms and Cell Cultures. They determined that this *Delftia* strain is electrochemically active, highlighting its ability to transfer electrons to external surfaces as a method of survival or persistence. These findings served as motivation to use the strain as a pure culture for testing in MFCs.

The MFCs chamber were assembled and then connected through a conduct with positive and negative charge towards. The data obtained were in millivolts, so it was possible to determine the power generation of the six cells for 15 days. At the end of the monitoring, the data reflected better results for the MFCs with maghemite compared to the MFCs that were only made up of carbon fiber. Figure 8 shows MFC 1-1 generated a direct current voltage of 152.81mV and the MFC 2-1 a voltage of 157.92 mV, being the lowest values compared to the other cells. Fig 8. shows MFC 1-1 generated a direct current voltage of 152.81mV and the MFC 2-1 a voltage of 157.92 mV, being the lowest values compared to the other cells. In contrast, when comparing the cells with carbon and maghemite (sample

B), showed that the MFC 1-2 presented a voltage of 236.18 mV and the MFC 2-2 of 258.12 mV and the cells with maghemite with heat treatment (sample A) had an improved voltage production reaching peaks of 284.74 mV in MFC 1-3 and 286.50mV in MFC 2-3.

In a previous study [59], it was determined that bioelectricity production in an MFC and the efficiency of COD removal are affected by the leachate percentage in the substrate. In the present study where 100% of the leachate was used, the bioelectricity production was similar to that obtained in a comparative study where the maximum production of bioelectricity was 152 mV [57]. On the other hand, the microbial biofilm affects the biodegradation of organic contaminants and bioelectricity production. In a study where biochar was used and compared with a gravel/sand surface, it was determined that bioelectricity production increases with a larger surface area [74]. Another study also reported similar findings [75]. With this precedent, our results reflect that adding maghemite to the carbon fiber membrane contributed to the increase in bioelectricity production, possibly because there was a larger contact surface for bacterial development. As far as we know, this material has not been tested in MFC membranes, so it could be an interesting alternative.

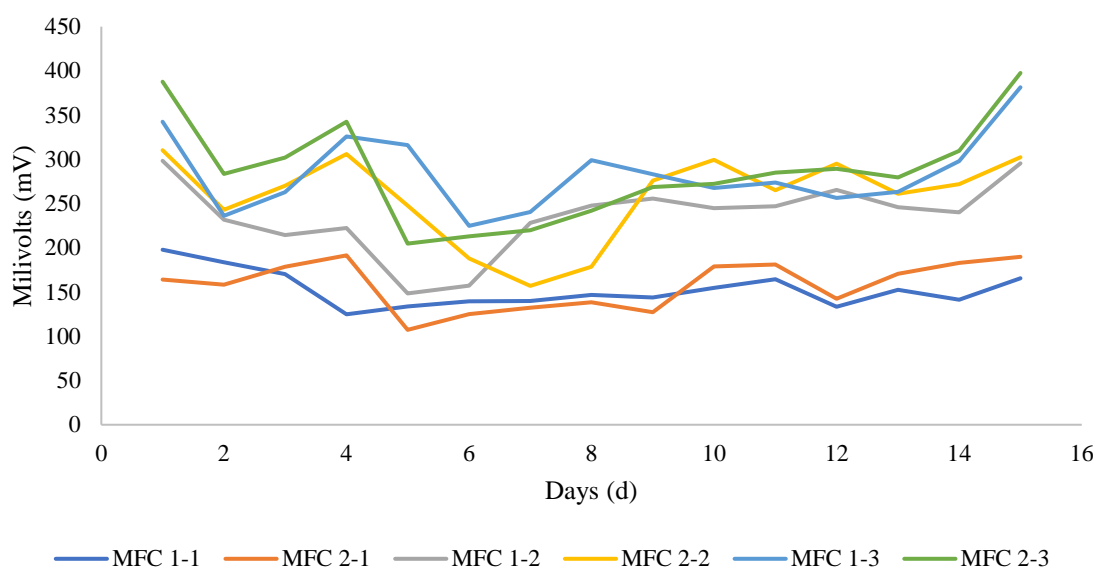


**Figure 8.** Voltages measured in MFCs. Treatment 1: cell with carbon fiber (repetition 1 MFC 1-1, repetition 2 MFC 2-1); Treatment 2: cell with carbon fiber + maghemite (repetition 1 MFC 1-2, repetition 2 MFC 2-2); Treatment 3: cell with carbon fiber + low heat treatment maghemite (repetition 1 MFC 1-3, repetition 2 MFC 2-3).

After checking the normality of the data, an ANOVA study was performed to compare the variances between the means of the three treatments in bioelectricity production and a p-value less than 0.05 was obtained, suggesting that there are significant differences between the treatments. Therefore, a Tukey test was conducted to generate a multiple comparison and determine which means are significantly different from others; the results are shown in Table 4 and Figure 9. In the lower half of Table 4, the estimated difference between each pair of means is displayed and asterisks have been placed next to three pairs to indicate statistically significant differences at a 95.0% confidence level. In the upper part of the Table, 3 homogeneous groups are identified by columns of “X”. Within each

column, the levels containing “X” form a group of means within which there are no statistically significant differences. The method used to discriminate between the means was Tukey's honest significant difference (HSD) procedure. With this method, there is a 5.0% risk of calling one or more pairs significantly different when their actual difference equals 0. Therefore, it is considered that there are significant differences between the three treatments and that applying a thermal treatment to maghemite contributes to higher bioelectricity production in microbial fuel cells.

**Table 4.** Tukey's Multiple Comparison Test.

| Method: 95.0 percent Tukey HSD |       |            |                    |
|--------------------------------|-------|------------|--------------------|
| Treatment                      | Count | Mean       | Homogeneous Groups |
| 3_1                            | 30    | 155.363    | X                  |
| 3_2                            | 30    | 247.149    | X                  |
| 3_3                            | 30    | 285.619    | X                  |
| Contrast                       | Sig.  | Difference | +/- Limits         |
| 3_1 - 3_2                      | *     | -91.7857   | 25.3553            |
| 3_1 - 3_3                      | *     | -130.255   | 25.3553            |
| 3_2 - 3_3                      | *     | -38.4697   | 25.3553            |

\* Denotes a statistically significant difference, Treatment 1 with carbon fiber: 3\_1; Treatment 2 cells with carbon fiber + maghemite: 3\_2; Treatment 3 cells with carbon fiber + low temperature treatment maghemite: 3-3

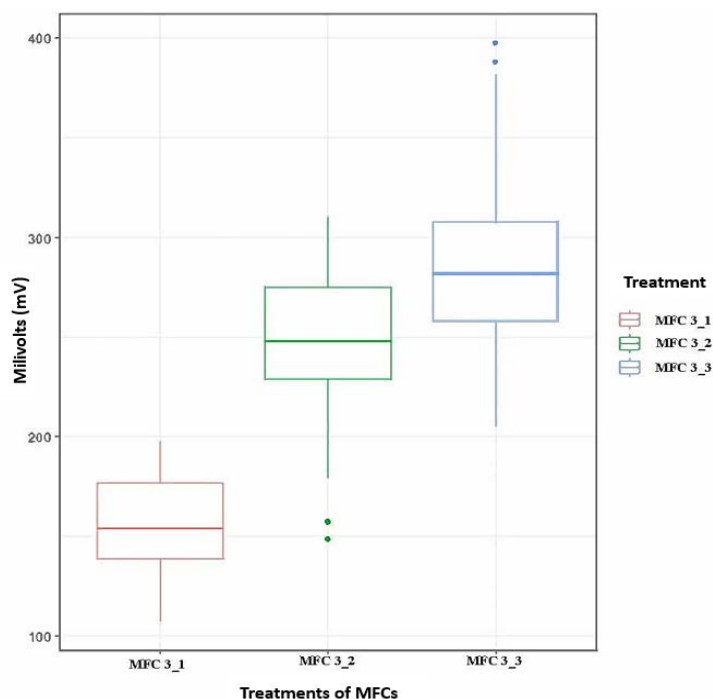


**Figure 9.** Box plot of MFCs. Treatment 1 cells with carbon fiber MFC 3\_1; Treatment 2 cells with carbon fiber + maghemite MFC 3\_2; Treatment 3 cells with carbon fiber + low temperature treatment maghemite MFC 3-3.

In this research, the use of maghemite nanoparticles and bacteria *Delftia acidovorans* in microbial fuel cells has been used as a synthetic material to improve bioelectricity production. According to [76],

the determination of microbial morphology of the model with maghemite nanoparticles shows interspecific electron transfer between bacteria, forming electroactive biofilms. Likewise, studies carried out by Nosek D et al. [71,77] allowed us to recognize that the different variations in the electrodes and reactors can have an important effect on the output power, bacterial growth and removal efficiency, mainly focused on the variations of the membranes can promote the simultaneous removal of carbon and nitrogen in the cells. Under these criteria, it was determined that the MFCs, when synthesized with maghemite nanoparticles, contributed to the performance of the cell due to the composition of iron oxides, increasing the interchange of electrons [78]. In the present study, the best bioelectricity production result was with a voltage up to 286.50mV for MFCs composed of heat-treated maghemite. The results obtained in the generation of bioelectricity using organic waste as a substrate are different compared to the results obtained in this research [79]. The importance of the *Delftia* bacterium in the degradation of leachate contaminants is emphasized, as supported by the findings in the genome sequencing study [67]. This study underscores *Delftia's* biodegradative capacity for contaminants such as polycyclic aromatic hydrocarbons (PAHs), compounds like N-heterocycles and pesticides.

However, additional studies are required to identify the exact mechanism that the bacteria employ for bioelectricity generation.

#### 4. Conclusions

This study compares bioelectricity production in six MFCs: two with a composite carbon fiber membrane, two with a maghemite membrane and two with low heat treated maghemite. In all cells, a pure culture of the bacterium *Delftia acidovorans* was used and 100% leachate–derived from fruit and vegetable waste–was added as the substrate.

In terms of contaminant removal, the treatment using carbon fiber demonstrated higher efficiency, achieving removal rates of up to 63.38% for BOD<sub>5</sub> and 69.67% for COD. This suggests that using carbon fiber as a proton exchange membrane is effective in purifying leachate contaminants. For the removal of ammonia nitrogen, all cells exhibited substantial efficiency, reaching up to 92.49%, with no significant differences observed among the three treatments. The pH value increased in all treatments due to the degradation of organic matter, registering a rise from 4.11 to 5.96 in the cell with low heat treated maghemite. Regarding bioelectricity production, cells employing maghemite as part of the proton exchange membrane yielded higher voltage, reaching values of up to 286.50 mV. Therefore, it can be inferred that the incorporation of maghemite in a membrane enhances the contact surface and promotes bioelectricity production. However, the efficiency of contaminant removal, including BOD<sub>5</sub> and COD, is impacted. Concerning the use of the bacterium *Delftia acidovorans*, its proficiency in thriving within an MFC and generating bioelectricity was demonstrated, yielding results comparable to other studies utilizing different bacterial consortia. However, further research is needed to elucidate its metabolic role in contaminant purification and electricity generation.

#### Use of AI tools declaration

The authors declare that AI tools were not used at all stages of research in the studies carried out and presented in this article.

## Acknowledgments

The authors we would like to express our utmost gratitude to all parties who have contributed to the successful implementation of this research. We would like to thank the research project "Opportunities and challenges of renewable energies as a territorial development in zones of the province of Chimborazo" funded by ESPOCH and its partner university, University of Saskatchewan, for all the financial and logistical support for the execution of this research. We would like to express our sincere gratitude to Dr. Zoltán Pásti to perform the XPS measurement. Dra. Szegedi Ágnes with the BET measurement and Dra. Mihaly Judith with the FTIR measurement.

## Conflicts of Interest

The authors declare no conflict of interest.

## References

1. Hersh B, Mirkouei A, Sessions J, et al. (2019) A Review and Future Directions on Enhancing Sustainability Benefits across Food-Energy-Water Systems: The Potential Role of Biochar-Derived Products. *AIMS Environ Sci* 6: 379–416. <https://doi.org/10.3934/environsci.2019.5.379>
2. Yang X, Chen S. (2021) Microorganisms in Sediment Microbial Fuel Cells: Ecological Niche, Microbial Response, and Environmental Function. *Sci. Total Environ* 756: 144145. <https://doi.org/10.1016/j.scitotenv.2020.144145>
3. Miramontes-Viña V, Romero-Castro N, López-Cabarcos M Á. (2023) Advancing towards a Sustainable Energy Model. Uncovering the Untapped Potential of Rural Areas. *AIMS Environ Sci* 10: 287–312. <https://doi.org/10.3934/environsci.2023017>
4. Srivastava R K, Boddula R, Pothu R. (2022) Microbial Fuel Cells: Technologically Advanced Devices and Approach for Sustainable/Renewable Energy Development. *Energy Convers Manag* X: 13: 100160. <https://doi.org/10.1016/j.ecmx.2021.100160>
5. Darmawan R, Juliastuti S R, Hendrianie N, et al. (2022) Effect of Electrode Modification on the Production of Electrical Energy and Degradation of Cr (VI) Waste Using Tubular Microbial Fuel Cell. *AIMS Environ Sci* 9: 505–525. <https://doi.org/10.3934/environsci.2022030>
6. Xin S, Shen J, Liu G, et al. (2022) Electricity Generation and Microbial Community of Single-Chamber Microbial Fuel Cells in Response to Cu<sub>2</sub>O Nanoparticles/Reduced Graphene Oxide as Cathode Catalyst. *Chem Eng J* 380: 122446. <https://doi.org/10.1016/j.cej.2019.122446>
7. Pant D, Van Bogaert G, Diels L, et al. (2010) A Review of the Substrates Used in Microbial Fuel Cells (MFCs) for Sustainable Energy Production. *Bioresour. Technol* 101: 1533–1543. <https://doi.org/10.1016/j.biortech.2009.10.017>
8. Guambo A, Calderón C, Paña S, et al. (2021) Bioelectricity Production with Organic Substrates, Nitrates and Lead Using High Andean Soils. *Adv Intell Syst Comput* 1277: 198–208. [https://doi.org/10.1007/978-3-030-60467-7\\_17](https://doi.org/10.1007/978-3-030-60467-7_17)
9. Arulmani S R B, Gnanamuthu H L, Kandasamy S, et al. (2021) Sustainable Bioelectricity Production from *Amaranthus Viridis* and *Triticum Aestivum* Mediated Plant Microbial Fuel Cells with Efficient Electrogenic Bacteria Selections. *Process Biochem* 107. <https://doi.org/10.1016/j.procbio.2021.04.015>



10. Nguyen H D, Babel S. (2023) A Novel Coupled Microbial Fuel Cell Operation for Organic and Nitrogen Removal with Simultaneous Energy Recovery from Wastewater. *Sustain Energy Technol Assessments* 55: 102981. <https://doi.org/10.1016/j.seta.2022.102981>
11. Bajracharya S. (2020) Microbial Fuel Cell Coupled with Anaerobic Treatment Processes for Wastewater Treatment. *Integr Microb Fuel Cells Wastewater Treat* 295–311. <https://doi.org/10.1016/B978-0-12-817493-7.00014-X>
12. Wrighton K C, Agbo P, Warnecke F, et al. (2008) A Novel Ecological Role of the Firmicutes Identified in Thermophilic Microbial Fuel Cells. *ISME J* 2: 1146–1156. <https://doi.org/10.1038/ismej.2008.48>
13. Zhang G, Feng S, Jiao Y, et al. (2017) Cathodic Reducing Bacteria of Dual-Chambered Microbial Fuel Cell. *Int J Hydrogen Energy* 42: 27607–27617. <https://doi.org/10.1016/j.ijhydene.2017.06.095>
14. Zhang G, Zhao Q, Jiao Y, et al. (2012) Biocathode Microbial Fuel Cell for Efficient Electricity Recovery from Dairy Manure. *Biosens Bioelectron* 31. <https://doi.org/10.1016/j.bios.2011.11.036>
15. Chen C Y, Chen T Y, Chung Y C A (2014) Comparison of Bioelectricity in Microbial Fuel Cells with Aerobic and Anaerobic Anodes. *Environ Technol* 35. <https://doi.org/10.1080/09593330.2013.826254>
16. Erensoy A, Mulayim S, Orhan A, et al. (2022) The System Design of the Peat-Based Microbial Fuel Cell as a New Renewable Energy Source: The Potential and Limitations. *Alexandria Eng J* 61: 8743–8750. <https://doi.org/10.1016/j.aej.2022.02.020>
17. Szydlowski L, Lan T C T, Shibata N, et al. (2020) Metabolic Engineering of a Novel Strain of Electrogenic Bacterium *Arcobacter Butzleri* to Create a Platform for Single Analyte Detection Using a Microbial Fuel Cell. *Enzyme Microb Technol* 139: 109564. <https://doi.org/10.1016/j.enzmictec.2020.109564>
18. Krithika T, Kavitha R, Dinesh M, et al. (2021) Assessment of Ligninolytic Bacterial Consortium for the Degradation of Azo Dye with Electricity Generation in a Dual-Chambered Microbial Fuel Cell. *Environ Challenges* 4: 100093. <https://doi.org/10.1016/j.envc.2021.100093>
19. Gupta P, Pandey K, Verma N. (2021) Improved Oxygen Reduction and Simultaneous Glyphosate Degradation over Iron Phthalocyanine and Reduced Graphene Oxide–dispersed Activated Carbon Fiber Electrodes in a Microbial Fuel Cell. *J Power Sources* 514. <https://doi.org/10.1016/j.jpowsour.2021.230592>
20. Ambaye T G, Vaccari M, Franzetti A, et al. (2023) Microbial Electrochemical Bioremediation of Petroleum Hydrocarbons (PHCs) Pollution: Recent Advances and Outlook. *Chem Eng J* 452. <https://doi.org/10.1016/j.cej.2022.139372>
21. Fatehbashar zad P, Aliasghari S, Tabrizi I S, et al. (2022) Microbial Fuel Cell Applications for Removal of Petroleum Hydrocarbon Pollutants: A Review. *Water Resour Ind* 28: 100178. <https://doi.org/10.1016/j.wri.2022.100178>
22. Puig S, Serra M, Coma M, et al. (2011) Microbial Fuel Cell Application in Landfill Leachate Treatment. *J Hazard Mater* 185. <https://doi.org/10.1016/j.jhazmat.2010.09.086>
23. Biffinger J C, Pietron J, Ray R, et al. (2007) A Biofilm Enhanced Miniature Microbial Fuel Cell Using *Shewanella Oneidensis* DSP10 and Oxygen Reduction Cathodes. *Biosens Bioelectron* 22: 1672–1679. <https://doi.org/10.1016/j.bios.2006.07.027>

24. Pu K B, Li T T, Gao J Y, et al. (2022) Floating Flexible Microbial Fuel Cells for Electricity Generation and Municipal Wastewater Treatment. *Sep Purif Technol* 300. <https://doi.org/10.1016/j.seppur.2022.121915>
25. Ghangrekar M M, Shinde V B. (2007) Performance of Membrane-Less Microbial Fuel Cell Treating Wastewater and Effect of Electrode Distance and Area on Electricity Production. *Bioresour Technol* 98: 2879–2885. <https://doi.org/10.1016/j.biortech.2006.09.050>
26. Xu J, Sheng G P, Luo H W, et al. (2012) Fouling of Proton Exchange Membrane (PEM) Deteriorates the Performance of Microbial Fuel Cell. *Water Res* 46: 1817–1824. <https://doi.org/10.1016/j.watres.2011.12.060>
27. Kondaveeti S, Lee J, Kakarla R, et al. (2014) Low-Cost Separators for Enhanced Power Production and Field Application of Microbial Fuel Cells (MFCs). *Electrochim Acta* 132: 434–440. <https://doi.org/10.1016/j.electacta.2014.03.046>
28. Li D, Feng Y, Li F, et al. (2023) Carbon Fibers for Bioelectrochemical: Precursors, Bioelectrochemical System, and Biosensors. *Adv Fiber Mater* 5: 699–730. <https://doi.org/10.1007/s42765-023-00256-w>
29. Shirvanimoghaddam K, Hamim S U, Akbari M K, et al. (2017) Carbon Fiber Reinforced Metal Matrix Composites: Fabrication Processes and Properties. *Compos. Part A Appl Sci Manuf* 92: 70–96. <https://doi.org/10.1016/j.compositesa.2016.10.032>
30. Oroumei A, Naebe M. (2017) Mechanical Property Optimization of Wet-Spun Lignin/Polyacrylonitrile Carbon Fiber Precursor by Response Surface Methodology. *Fibers Polym* 18. <https://doi.org/10.1007/s12221-017-7363-9>
31. Djellali M, Kameche M, Kebaili H, et al. (2021) Synthesis of Nickel-Based Layered Double Hydroxide (LDH) and Their Adsorption on Carbon Felt Fibres: Application as Low Cost Cathode Catalyst in Microbial Fuel Cell (MFC). *Environ Technol* 42. <https://doi.org/10.1080/09593330.2019.1635652>
32. Li X, Liu G, Ma F, et al. (2018) Enhanced Power Generation in a Single-Chamber Dynamic Membrane Microbial Fuel Cell Using a Nonstructural Air-Breathing Activated Carbon Fiber Felt Cathode. *Energy Convers Manag* 172. <https://doi.org/10.1016/j.enconman.2018.07.011>
33. Jiang D, Chen H, Xie H, et al. (2023) Fe, N, S Co-Doped Cellulose Paper Carbon Fibers as an Air-Cathode Catalyst for Microbial Fuel Cells. *Environ Res* 221. <https://doi.org/10.1016/j.envres.2023.115308>
34. Yan S, Xiong W, Xing S, et al. (2017) Oxidation of Organic Contaminant in a Self-Driven Electro/Natural Maghemite/Peroxydisulfate System: Efficiency and Mechanism. *Sci Total Environ* 599–600. <https://doi.org/10.1016/j.scitotenv.2017.05.037>
35. Khalifa A Y Z, Almalki M. (2019) Polyphasic Characterization of Delftia Acidovorans ESM-1, a Facultative Methylotrophic Bacterium Isolated from Rhizosphere of Eruca Sativa. *Saudi J Biol Sci* 26. <https://doi.org/10.1016/j.sjbs.2018.05.015>
36. Chen Y L, Lee C C, Lin Y L, et al. (2015) Obtaining Long 16S rDNA Sequences Using Multiple Primers and Its Application on Dioxin-Containing Samples. *BMC Bioinformatics* 16: S13. <https://doi.org/10.1186/1471-2105-16-S18-S13>
37. Geer L Y, Marchler-Bauer A, Geer R C, et al. (2009) The NCBI BioSystems Database. *Nucleic Acids Res* 38. <https://doi.org/10.1093/nar/gkp858>
38. Meeker E W, Wagner E C (1933) Titration of Ammonia in Presence of Boric Acid. *Ind Eng Chem Anal Ed* 5: 396–398. doi:10.1021/ac50086a012. <https://doi.org/10.1021/ac50086a012>

39. Standard Methods For the Examination of Water and Wastewater 5210 BIOCHEMICAL OXYGEN DEMAND (BOD). *Stand Methods Exam Water Wastewater* doi:10.2105/SMWW.2882.102.
40. Wastewater, S.M.F. the E. of W. and 5220 CHEMICAL OXYGEN DEMAND (COD). *Stand. Methods Exam. Water Wastewater* .
41. Wastewater, S.M.F. the E. of W. and 4500-H+ PH. *Stand. Methods Exam. Water Wastewater*.
42. Zhang C F, Zhong X C, Yu H Y, et al. (2009) Effects of Cobalt Doping on the Microstructure and Magnetic Properties of Mn-Zn Ferrites Prepared by the Co-Precipitation Method. *Phys B Condens Matter* 404: 2327–2331. <https://doi.org/10.1016/j.physb.2008.12.044>
43. Silva C, Borbáth I, Zelenka K, et al. (2022) Effect of the Reductive Treatment on the State and Electrocatalytic Behavior of Pt in Catalysts Supported on Ti<sub>0.8</sub>Mo<sub>0.2</sub>O<sub>2</sub>-C Composite. *React Kinet Mech Catal* 135: 29–47. <https://doi.org/10.1007/s11144-021-02131-4>
44. Pászti Z, Hakkell O, Keszthelyi T, et al. (2010) Interaction of Carbon Monoxide with Au(111) Modified by Ion Bombardment: A Surface Spectroscopy Study under Elevated Pressure. *Langmuir* 26: 16312–16324. <https://doi.org/10.1021/la1014913>
45. N. Fairley CasaXPS: Spectrum Processing Software for XPS, AES and SIMS. Cheshire.
46. Diczházi D, Borbáth I, Bakos I, et al. (2021) Design of Mo-Doped Mixed Oxide–Carbon Composite Supports for Pt-Based Electrocatalysts: The Nature of the Mo-Pt Interaction. *Catal Today* 366: 31–40. <https://doi.org/10.1016/j.cattod.2020.04.004>
47. Mohai, M. XPS MultiQuant: Multi-Model X-Ray Photoelectron Spectroscopy Quantification Program. Version 7.00.92. **2011**.
48. Mohai, M. XPS MultiQuant: Multimodel XPS Quantification Software. *Surf Interface Anal* 36: 828–832. <https://doi.org/10.1002/sia.1775>
49. Zhang J, Li J, Ye D, et al. (2014) Enhanced Performances of Microbial Fuel Cells Using Surface-Modified Carbon Cloth Anodes: A Comparative Study. *Int J Hydrogen Energy* 39: 19148–19155. <https://doi.org/10.1016/j.ijhydene.2014.09.067>
50. Feng Y, Yang Q, Wang X, et al. (2010) Treatment of Carbon Fiber Brush Anodes for Improving Power Generation in Air–Cathode Microbial Fuel Cells. *J Power Sources* 195: 1841–1844. <https://doi.org/10.1016/j.jpowsour.2009.10.030>
51. Karami M, McMorrow G V, Wang L (2018) Continuous Monitoring of Indoor Environmental Quality Using an Arduino-Based Data Acquisition System. *J Build Eng* 19. <https://doi.org/10.1016/j.jobe.2018.05.014>
52. Escapa A, Gil-Carrera L, García V, et al. (2012) Performance of a Continuous Flow Microbial Electrolysis Cell (MEC) Fed with Domestic Wastewater. *Bioresour Technol* 117.
53. Nanda A, Mohapatra B B, Mahapatra A P K, et al. (2021) Multiple Comparison Test by Tukey’s Honestly Significant Difference (HSD): Do the Confident Level Control Type I Error. *Int J Stat Appl Math* 6. <https://doi.org/10.22271/math.2021.v6.i1a.636>
54. Feng S, Hou S, Huang X, et al. (2019) Insights into the Microbial Community Structure of Anaerobic Digestion of Municipal Solid Waste Landfill Leachate for Methane Production by Adaptive Thermophilic Granular Sludge. *Electron J Biotechnol* 39. <https://doi.org/10.1016/j.ejbt.2019.04.001>
55. Ghosh P, Gupta A, Thakur I S. (2015) Combined Chemical and Toxicological Evaluation of Leachate from Municipal Solid Waste Landfill Sites of Delhi, India. *Environ Sci Pollut Res* 22. <https://doi.org/10.1007/s11356-015-4077-7>

56. MAE TULSMA Available online: <https://www.ambiente.gob.ec/wp-content/uploads/downloads/2018/05/TULSMA.pdf> (accessed on 2 October 2023).
57. Saeed T, Yadav A K, Miah M J (2022) Landfill Leachate and Municipal Wastewater Co-Treatment in Microbial Fuel Cell Integrated Unsaturated and Partially Saturated Tidal Flow Constructed Wetlands. *J Water Process Eng* 46. <https://doi.org/10.1016/j.jwpe.2022.102633>
58. Kumar S S, Kumar A, Malyan S K, et al. (2023) Landfill Leachate Valorization: A Potential Alternative to Burden off Resources and Support Energy Systems. *Fuel* 331. <https://doi.org/10.1016/j.fuel.2022.125911>
59. Hassan M, Wei H, Qiu H, et al. (2018) Power Generation and Pollutants Removal from Landfill Leachate in Microbial Fuel Cell: Variation and Influence of Anodic Microbiomes. *Bioresour Technol* 247. <https://doi.org/10.1016/j.biortech.2017.09.124>
60. Li X, Lu Y, Luo H, et al. (2021) Effect of PH on Bacterial Distributions within Cathodic Biofilm of the Microbial Fuel Cell with Maltodextrin as the Substrate. *Chemosphere* 265. <https://doi.org/10.1016/j.chemosphere.2020.129088>
61. Singh M, Ulbrich P, Prokopec V, et al. (2013) Vapour Phase Approach for Iron Oxide Nanoparticle Synthesis from Solid Precursors. *J Solid State Chem* 200: 150–156. <https://doi.org/10.1016/j.jssc.2013.01.037>
62. Asuha S, Zhao Y M, Zhao S, et al. (2012) Synthesis of Mesoporous Maghemite with High Surface Area and Its Adsorptive Properties. *Solid State Sci* 14: 833–839. <https://doi.org/10.1016/j.solidstatesciences.2012.04.011>
63. Trushkina Y, Tai C W, Salazar-Alvarez G. (2019) Fabrication of Maghemite Nanoparticles with High Surface Area. *Nanomaterials* 9. <https://doi.org/10.3390/nano9071004>
64. Guivar J A R, Sadrollahi E, Menzel D, et al. Magnetic, Structural and Surface Properties of Functionalized Maghemite Nanoparticles for Copper and Lead Adsorption. *RSC Adv* 7: 28763–28779, <https://doi.org/10.1039/C7RA02750H>
65. Patekari M D, Pawar K K, Salunkhe G B, et al. (2021) Synthesis of Maghemite Nanoparticles for Highly Sensitive and Selective NO<sub>2</sub> Sensing. *Mater Sci Eng B Solid-State Mater Adv Technol* 272: 115339. <https://doi.org/10.1016/j.mseb.2021.115339>
66. Cao D, Li H, Pan L, et al. High Saturation Magnetization of  $\gamma$ -Fe<sub>2</sub>O<sub>3</sub> Nano-Particles by a Facile One-Step Synthesis Approach. *Sci Rep* 6: 1–9. <https://doi.org/10.1038/srep32360>
67. Shetty A R, de Gannes V, Obi C C, et al. (2015) Complete Genome Sequence of the Phenanthrene-Degrading Soil Bacterium *Delftia Acidovorans* Cs1-4. *Stand Genomic Sci* 10. <https://doi.org/10.1186/s40793-015-0041-x>
68. Morel M A, Ubalde M C, Braña V, et al. (2011) *Delftia* Sp. JD2: A Potential Cr(VI)-Reducing Agent with Plant Growth-Promoting Activity. *Arch Microbiol* 193. <https://doi.org/10.1007/s00203-010-0632-2>
69. Leibelng S, Schmidt F, Jehmlich N, et al. (2010) Declining Capacity of Starving *Delftia Acidovorans* MC1 to Degrade Phenoxypropionate Herbicides Correlates with Oxidative Modification of the Initial Enzyme. *Environ Sci Technol* 44. <https://doi.org/10.1021/es903619j>
70. Morel M A, Iriarte A, Jara Tellechea E S, et al. (2016) Revealing the Biotechnological Potential of *Delftia* Sp. JD2 by a Genomic Approach. *AIMS Bioeng* 3: 156–175. <https://doi.org/10.3934/bioeng.2016.2.156>

71. Nosek D, Samsel O, Pokój T, et al. (2023) Waste Volatile Fatty Acids as a Good Electron Donor in Microbial Fuel Cell with the Iron-Modified Anode. *Int J Environ Sci Technol* 20. <https://doi.org/10.1007/s13762-023-04850-8>
72. Ishii S, Logan B E, Sekiguchi Y. (2012) Enhanced Electrode-Reducing Rate during the Enrichment Process in an Air-Cathode Microbial Fuel Cell. *Appl Microbiol Biotechnol* 94. <https://doi.org/10.1007/s00253-011-3844-8>
73. Jangir Y, French S, Momper L M, et al. (2016) Isolation and Characterization of Electrochemically Active Subsurface Delftia and Azonexus Species. *Front Microbiol* 7. <https://doi.org/10.3389/fmicb.2016.00756>
74. Malyan S K, Kumar S S, Fagodiya R K, et al. (2021) Biochar for Environmental Sustainability in the Energy-Water-Agroecosystem Nexus. *Renew. Sustain. Energy Rev* 149: 111379. <https://doi.org/10.1016/j.rser.2021.111379>
75. Saeed T, Miah M J, Yadav A K (2022) Development of Electrodes Integrated Hybrid Constructed Wetlands Using Organic, Construction, and Rejected Materials as Filter Media: Landfill Leachate Treatment. *Chemosphere* 303. <https://doi.org/10.1016/j.chemosphere.2022.135273>
76. Vu M T, Noori M T, Min B. (2020) Magnetite/Zelite Nanocomposite-Modified Cathode for Enhancing Methane Generation in Microbial Electrochemical Systems. *Chem Eng J* 393. <https://doi.org/10.1016/j.cej.2020.124613>
77. Omid M, Mashkour M, Biswas J K, et al. (2021) From Electricity to Products: Recent Updates on Microbial Electrosynthesis (MES). *Top Catal* <https://doi.org/10.1007/s11244-021-01503-3>
78. Liu P, Liang P, Jiang Y, et al. (2018) Stimulated Electron Transfer inside Electroactive Biofilm by Magnetite for Increased Performance Microbial Fuel Cell. *Appl Energy* 216. <https://doi.org/10.1016/j.apenergy.2018.01.073>
79. Nouri P, Najafpour Darzi G. (2017) Impacts of Process Parameters Optimization on the Performance of the Annular Single Chamber Microbial Fuel Cell in Wastewater Treatment. *Eng Life Sci* 17 <https://doi.org/10.1002/elsc.201600173>



AIMS Press

© 2023 the Author(s), licensee AIMS Press. This is an open access article distributed under the terms of the Creative Commons Attribution License (<http://creativecommons.org/licenses/by/4.0>)